



BCSIR

Available online at [www.banglajol.info](http://www.banglajol.info)

Bangladesh J. Sci. Ind. Res. 49(3), 147-154, 2014

**BANGLADESH JOURNAL  
OF SCIENTIFIC AND  
INDUSTRIAL RESEARCH**

E-mail: [bjisir07@gmail.com](mailto:bjisir07@gmail.com)

## Performance Evaluation of a low cost integrated collector storage solar water heater with independent plane reflectors

Zakariya Kaneesamkandi\*

*Department of Mechanical Engineering, College of Engineering, King Saud University, Riyadh-11421, Saudi Arabia.*

### Abstract

High initial cost is one of the reasons why consumers think twice before investing on the conventional solar water heating systems, especially in low income countries. Integrated collector storage systems are available at a lesser cost, but with a penalty of decreased efficiency. In this paper, yet another attempt to reduce cost of solar water heating system has been made by using independent plane reflectors along with an insulated storage tank provided with a heat absorbing aperture. With no tracking arrangement, this system uses only the intense beam radiation available from 9:00 AM to 3:00 PM with a concentration factor of 10. A theoretical study was conducted using commercial computational fluid dynamics software which was followed by an experimental validation of the results. The theoretical results were in agreement with the experimental results. The efficiency of this system was less than collector storage systems reported in the literature by about 10-15%. Maximum average tank temperature of 350 K and efficiency of 0.61 was obtained. Overall loss coefficient was identical with that of existing integrated collector storage systems.

**Keywords:** Solar energy; Energy storage; Integrated collector storage; Concentrating collector

### Introduction

Solar water heating systems are usually classified into active and passive systems based on whether external energy is used to drive the fluid within the system. Conventional passive water heating systems use tubes embedded in the collector plate along with glazing and water flows from the collector into the storage tank by thermo-siphon effect. Tubes, insulation material and weather resistant glass apart from storage tank and interconnecting piping escalate the cost of the system. Integrated collector storage systems (ICS) were developed as a cheaper alternative and these are passive solar collectors that use a storage tank which also acts as the absorber of the solar radiation. They are much cheaper to make compared to the conventional flat plate collectors. The solar radiation falling on the collector storage tank could be direct radiation or reflected radiation or both. The earliest model of the ICS system incorporated a simple tank which was painted black in order to increase the heat gain and left to itself. Increased heat losses in these systems especially during the night necessitated several improvements and many of these have been periodically reported in the literature. A complete review of the different types of integrated collector storage solar water heating systems is made by Smyth and Co-workers (Smyth *et al.*, 2006). A discussion of different types of integrated passive

water heaters giving their principle of working is made by David Bainbridge, (1981).

Advantages of ICS systems include low cost of manufacture and installation, absence of pumps or controls, simple construction, long lasting performance and absence of freezing problem usually encountered in thermo-siphon units which use small tubes. Disadvantages of ICS systems are reduced efficiency levels, higher heat losses and lower maximum attainable temperatures compared to conventional flat plate collectors. However, higher cost of flat plate collectors and its non-affordability in the developing and under developed countries requires that ICS systems with better efficiency and lower cost should be developed.

A report on the performance of an ICS system with collector-storage tank enclosed in a concentrating parabolic dish which also acts as the reflector is made by Helal and Co-workers. (Helal *et al.* 2010). Maximum temperature of 600C is obtained. They reported a maximum mean daily efficiency of 0.69 with the system facing southwest direction. The performance of a roof mounted ICS system of 114 liter capacity used along with a gas fired heating system is reported (Eve Commerford *et al.*, 2008). Higher heat transfer coefficient and stratification effect is reported

\*Corresponding author: E-mail: [zkaneesamkandi@ksu.edu.sa](mailto:zkaneesamkandi@ksu.edu.sa)

(Sridhar and Reddy, 2007) who conducted a numerical study and experimental validation of the transient performance of modified cuboids shaped ICS. Corrugated absorber surface on a plane ICS system without concentrators is reported to have increased temperature rise (Rakesh and Rosen, 2010). However, no advantage of the stratification effect is obtained due to the heat flow from the top of the collector. Heat input from below the tank can help to achieve better efficiency because of the stratification effect in the tank. Experiments on single as well as double tank ICS systems with tanks placed in enclosures with curved reflectors is reported by Tripanagnostopoulos and Souliotis, 2004. Results indicated that horizontal tank arrangement gave a better thermal performance and satisfactory temperature rise. A numerical study of this type of system using k- $\epsilon$  model is made by Moni and co-workers (Monia *et al*, 2011), in which agreement with experiments was obtained. A numerical model for evaluating the performance of ICS systems is developed (Hamdi *et al*, 2013). The model is applicable for fully enclosed ICS systems and comparison of temperature measurements with theoretical values differed by less than 1.5%. Experimental performance of ICS consisting of a twin cylinder storage tank with the annular spacing evacuated to prevent heat loss is reported. (Souliotis, 2011). Loss coefficient of the system was similar to that of flat plate collectors. In all these systems, attention is focused on the arrangement of the storage tank.

The present study deals with an exposed ICS system in which an independent horizontally placed solar collector cum storage tank receives reflected solar radiation from a series of plane reflectors. In this system, the reflectors are independent and located away from the collector storage tank. This is different from the usual method in which the reflectors are integrated with the collector storage tank. The important features of this system are its simplicity, easy installation and low cost. Since the reflected radiation is incident on the bottom side of the tank, stratification effect is utilized for better thermal efficiency. A numerical model is constructed to simulate the natural convective heat transfer within the tank and the results are compared with those of the prototype. Analysis of results and the performance characteristics indicate similar performance comparable with existing ICS systems.

The following are the objectives of the study:

- To make a theoretical study of the ICS system with the help of a commercial CFD software
- To conduct experiments on the system and determine the temperature profile and efficiency
- To compare the theoretical and experimental results and consolidate the system performance

### System description

Figures (1)a and (1)b give the experimental set up and the tank description respectively. The axis of the tank is placed along the east-west direction in the direction of movement of the sun. The central receiver tank made of galvanized steel sheet is 0.5m in diameter and 0.75m long with a capacity of 147.18 liters. The tank is surrounded by a 0.05m thick polystyrene insulation and enclosed within a polyvinyl chloride (PVC) drum of 5 mm thickness. The two circular ends of the tank are also insulated. The lower part of the tank is exposed to the reflected radiation from the rectangular mirrors. The included angle of the linearly exposed region is 300 at the centre of the tank. The exposed area is painted with lamp black in order to maximize heat absorption by the tank. The axis of the tank is 0.8m above the ground level. The five reflecting mirrors of size 1m x 0.15m each are arranged on either side of the tank near the floor level and they are oriented to reflect beam radiation to the exposed region at the bottom the tank.

### Methodology

The system is designed such that solar radiation is reflected towards the absorber between 9 AM and 3 PM during which time, the intensity of solar radiation is the

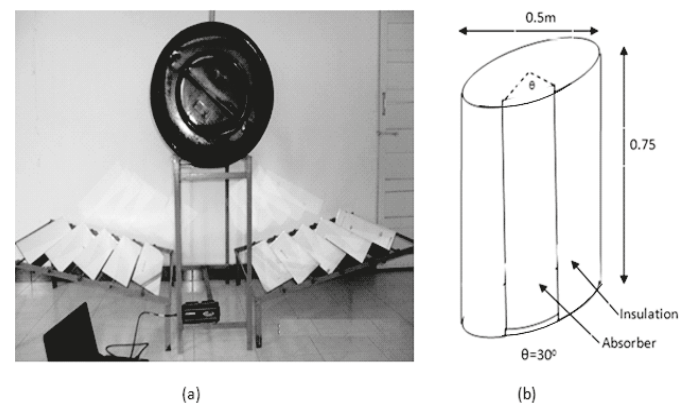


Fig. 1. (a) The experimental set up showing the central receiver cum storage tank along with the reflecting mirrors  
(b) The description of the ICS tank.

maximum. The reflectors were located independently as against the conventional method of integrating the reflecting surfaces within the collection system. The angle of incidence of solar beam radiation with the normal to the reflecting mirrors,  $\theta$ , at a particular time of the day, represented by  $t$ , on a particular day of the year, represented by  $n$ , can be estimated from equation 1 given below (Sukatme, 2002).

$$\cos(\theta) = [\sin(\delta) \times \sin(\phi - \beta)] + [\cos(\delta) \times \cos(\omega) \times \cos(\phi - \beta)] \dots \dots \dots (1)$$

$$I_b = I_n \times \cos\theta \dots \dots \dots (3)$$

$\delta$  – Declination angle which is given by the following relationship (Equation 2):

$$I_n = A \times \exp(-B / \sin \beta)$$

$$\delta = 23.45 \times \sin[(360 / 265) \times (284 + n)] \dots \dots \dots (2)$$

$\theta$  is the angle of incidence, A is the apparent solar-radiation constant, B is the atmospheric extinction coefficient, and  $\beta$  is the solar altitude angle above the horizontal, Table 1.

$\phi$ - Latitude of the location

The value of  $\sin \beta$  is calculated using equation 4 given below.

$\beta$  - Angle of tilt of the reflector with reference to the ground

$$\sin(\beta) = [\sin(\phi) \times \sin(\delta)] + [\cos(\phi) \times \cos(\delta) \times \cos(\omega)] \dots \dots \dots (4)$$

$\omega$ - Hour angle which is equivalent to 15 $\omega$  for every hour starting from -1800 to +1800 beginning from 12 noon.

**Table 1. Apparent radiation constant and atmospheric extinction coefficient**

The location chosen for the experiment is Riyadh, Saudi Arabia where the latitude is 24.63 $^{\circ}$  north. The corresponding values of the angle of incidence are +45.70 $^{\circ}$  at 9 AM and -45.70 $^{\circ}$  at 3 PM as illustrated in figure 2(a). It can be observed that the absorber surface receives the reflected radiation from the mirrors over 75% of its area starting from 9 AM which increases to 100% at noon and again reduces to 75% at 3 PM.

Month	A	B	C	$\Delta$
Jan	1230	0.142	0.058	-20.0
July	1085	0.207	0.136	-20.6

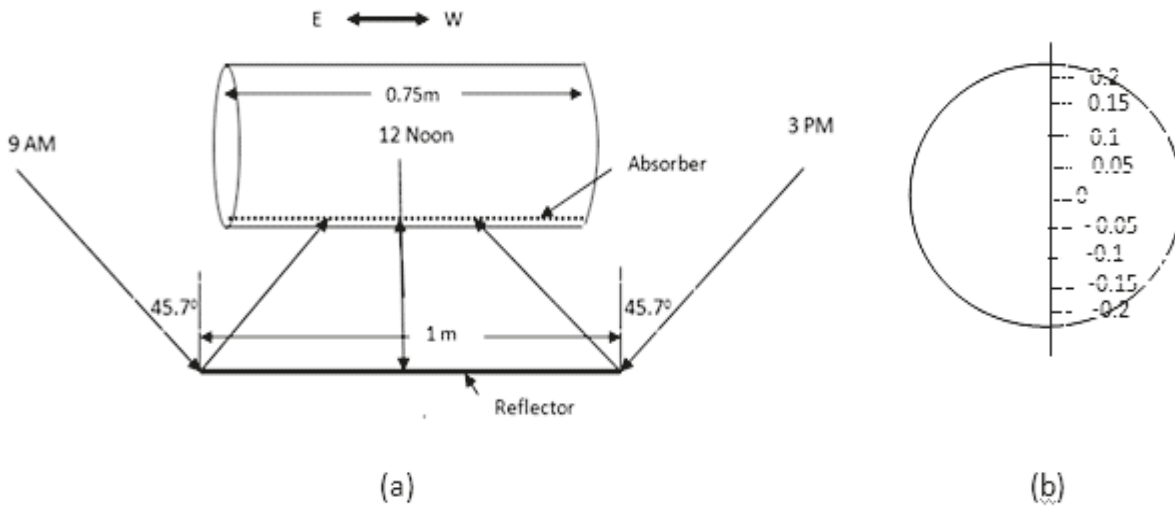


**Fig. 2. (a) Angle of incident and reflected beam radiation at 9 AM, 12 Noon and 3 PM (b) Points of temperature measurement in the tank in meters from center**

The ambient temperature, absorber surface temperature and water temperature at the tank at different points as shown in Fig.2 (b) are recorded with the help of the data acquisition system during the day.

The mean daily system efficiency is calculated using equation 5 given below:

The intensity of mean hourly beam radiation is obtained by using equation 3 (Sanea *et al*, 2004).

$$\eta = \frac{[F_R \times A \times \{I - (U_L \times T_{md})\}]}{[A \times I]} = F_R - \left( \frac{F_R \times U_L \times T_{md}}{I} \right) \dots \dots \dots (5)$$

$\eta$  is the mean daily efficiency

$F_R$  is the heat removal factor

$A$  is the absorber area

$I$  is the radiation incident on the absorber surface

$U_L$  is the overall heat transfer coefficient

$T_{md}$  is the mean daily temperature

The mean daily efficiency,  $\eta$  is determined as a function of the ratio  $T_{md} / I$  where  $T_{md}$  is the mean daily temperature given by  $[(T_f+T_i) / 2] - T_{am}$  where  $T_{am}$  is the mean ambient temperature. The overall loss coefficient,  $U_L$ , of the system was determined from this data by graphically determining the values of  $F_r$  and  $(F_r.U_L)$ . The thermal loss coefficient for the storage tank during the night,  $U_s$ , is given by the Eq.6.

$$U_s = \left[ \frac{\rho \times C_p}{\Delta t} \ln \left\{ \frac{(T_i - T_{am})}{(T_f - T_{am})} \right\} \right] \dots \dots \dots (6)$$

$\rho$  is the density of water

$C_p$  is the specific heat of water

$T_i$  is the initial temperature of water in the tank after 3:00 PM

$T_f$  is the final temperature of water in the tank after 3:00 PM

$T_{am}$  is the mean ambient temperature during the storage period

$\Delta t$  is the storage time in seconds from 3:PM to 9:00 AM

The methodology of study involves a theoretical modeling in which the model of the collector cum storage tank was made and simulated using the CFD package. This is followed by the experimental study and comparison of the results.

*Assumptions*

The following assumptions are made in this study:

1. The beam radiation falling on the reflector surfaces is a constant fraction of the measured global radiation intensity.
2. Heat is received by the absorber from 9:00 AM to 3:00 PM. The radiation received outside these times are not

considered for the simulation. However, this would have a negligible impact on the experimental data since a small quantity of solar radiation is reflected on the absorber before and after this specified time also.

3. The reflectivity of the mirrors is considered as unity.
4. Wind velocity effects on the absorber surface is not considered since the area is small and surrounded by the insulation layer covering the remaining portion of the tank.

*Performance modeling:*

A transient performance simulation of the above integrated collector cum storage tank was done using the commercial CFD package. The tank is under static condition with no mass flow inlet or outlet. Heat flows into the tank from the

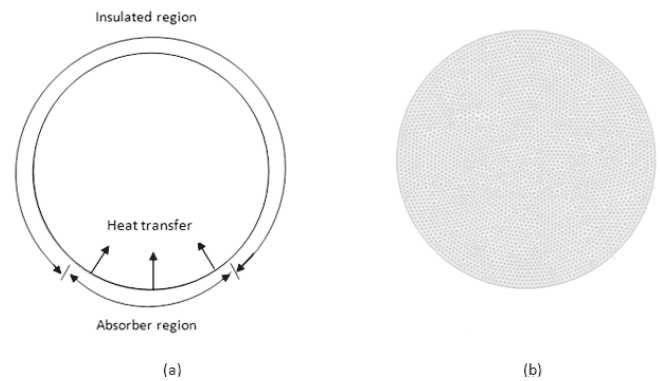


**Fig. 3. (a) The outline of the model (b) Two dimensional triangular mesh**

absorber region at the bottom of the tank as described above. The remaining areas of the tank are insulated and an ideal case of no heat loss is assumed in these walls. A two dimensional model with triangular meshing is done as shown in Fig. 3(a) and Fig. 3(b). The mesh size is 7222 cells.

Transient CFD calculations were performed with a water density as function of temperature. The PRESTO and second order upwind methods were used for the discretization of the pressure and momentum/energy equations. The SIMPLE algorithm is used to treat the pressure-velocity coupling. Transient simulations started from a uniform tank temperature of 300 K. The calculation is considered as convergent for the continuity equation, the momentum equations and the energy equation. The simulation was run with a time step of 1 s. After the configuration of the computational domain, the boundary and initial conditions were given. The energy balance equation is enabled and water properties are set via the Boussinesq natural

convection. The entire domain is set to an initial temperature of 300 K. Also the convective heat transfer boundary condition is set using the “Boundary Conditions” panel. The tank wall is specified as adiabatic wall. For natural convection gravity is enabled. The gravitational acceleration is set to 9.81m/s<sup>2</sup> in the negative y-direction.

The buoyancy for an incompressible fluid with constant fluid properties is modelled by using the Boussinesq approximation. The model uses a constant density fluid model but applies a local gravitational body force throughout the physical domain which is a linear function of the fluid thermal expansion coefficient ( $\beta$ ) and the local temperature difference relative to a datum called the buoyancy reference temperature. The Boussinesq approximation models the change in density using Eq. 7.

$$(\rho - \rho_r) = -\rho_r \times \beta \times (T - T_r) \dots \dots \dots (7)$$

T is the local temperature in K,

T<sub>r</sub> is the buoyancy reference temperature in K,

$\beta$  is the thermal expansion coefficient taken as 0.0002 K<sup>-1</sup>

$\rho_r$  is the density of water in kg/m<sup>3</sup> and

$\rho$  is the local density in kg/m<sup>3</sup>

**Experiments**

Experimental data of the ICS system performance was obtained by measuring temperatures and solar radiation intensity. The tank was aligned in the east west direction in order to ensure that all the solar radiation falling on the mirror surface are reflected directly to the absorber during



Fig. 4. Beam radiation intensity falling on the reflectors from 9:00 AM to 3:00 PM.

the complete period of operation, that is, 9 AM to 3 PM. Due to high incidence angle during the early and later hours of the day, reflected radiation fall outside the absorber during these times. However, the design and layout ensures that 75% of the reflected solar radiation starts falling on the absorber surface by 9.00 AM. This increases to 100% at mid day and starts decreasing to 75% up to 3 PM. A 32 channel (16 differential input) data acquisition system was programmed to collect ten temperature samples and one solar radiation intensity sample every 10 minutes. Fig.2 (b) gives the points where temperature sensors are located inside the storage tank. The sensors used were K type thermocouples. These nine sensors are provided to measure the water temperatures at different heights inside the tank. Another temperature sensor was used to measure the ambient temperature. A pyranometer was connected in order to record the intensity of total solar radiation falling on the reflectors. The input from the pyranometer was converted to beam radiation level by using a factor of 0.865 by adopting the trend in theoretical beam and diffuse solar radiation data as given by Sanea *et al*, 2004. The beam radiation data thus obtained is given in Fig.4.

**Results and discussion**

The results of the simulation of the ICS system were obtained for three different times, namely, after 10 minutes, 180 minutes and 360 minutes. Temperature contours and the temperature profile plots at these times are given in Fig. 5, 6 and 7. The contours indicate the temperature rise in the tank along with the convective movement. The absorber surface and its neighborhood possesses the maximum temperature. This around 357 K after 10 min of operation (Fig.5a) and the minimum water temperature is 300 K. Fig.5b gives the distribution of temperatures at different heights within the tank. It shows that the maximum temperatures are limited to the region between -0.25m and -0.2m. The region between -0.2m and 0.05m is at the temperature range of 300K to 320K during this time. The region between 0.05 and 0.25m is at 300K. Fig.6a gives the temperature contours after 3 hours of operation. Fig.6b gives the temperature distribution in the tank after 3 hours of operation. It is seen that the maximum temperature at the absorber surface is 400 K and the minimum water temperature in the tank has reached 335 K. The region of the tank between -0.2 to -0.05 has reached the temperature range of 205-350K and the region between -0.05m and 0.25m has reached temperatures range of 305-340K. Fig. 7a gives the temperature contours after 6 hours of operation. The absorber surface temperature is at 415K and the minimum water temperature is at 343K. The temperature distribution plot indicates that the region between -0.15m

and 0.05m have temperatures ranging from 360K to 375K. The region between 0.05m and 0.25m has temperatures between 340 and 350K. Fig.7b gives the static temperature plot.

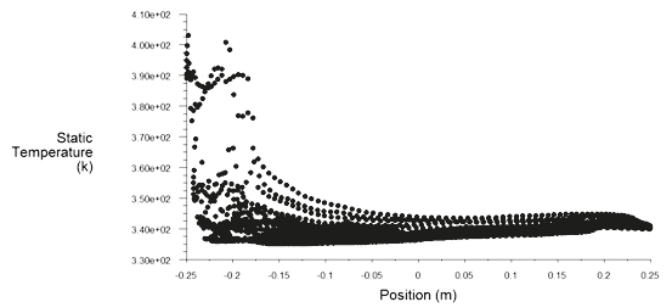
The temperature rise of the water in the tank at different levels with the time starting from 9:00AM is given in Fig. 8. It can be seen that level -0.20m and -0.15m have distinct values of temperature rise but the other levels overlap each other with terminal values in the range of 345-350K. This is in agreement with the temperature contours obtained from

$$\eta = 0.6134 - 6.6235 \times \left( \frac{T_{md}}{I_a} \right) \dots\dots\dots (8)$$

the simulation results. It is also observed that the water temperature reaches 330-340K within the first 100 minutes of operation after which the rate of temperature rise is retarded. Fig.9 gives the comparison of the experimental and the model simulation results. It is evident that the

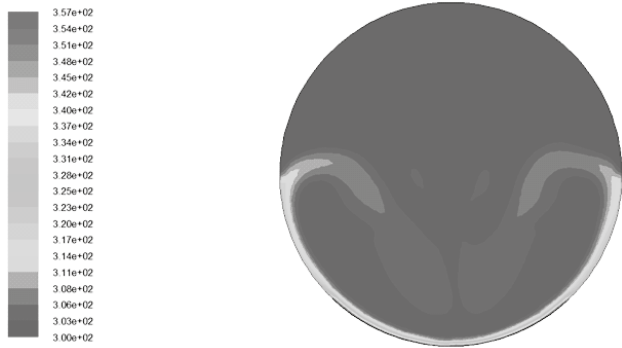


(a)

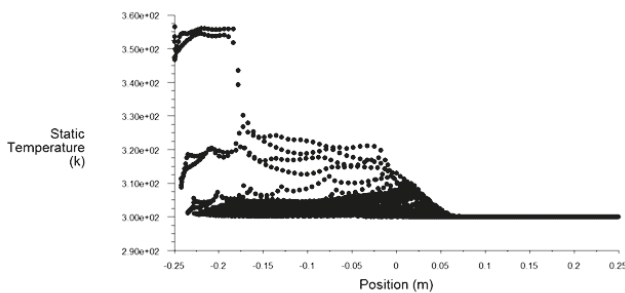


(b)

Fig. 6. (a) Temperature contours inside the tank after 3 hours (b) Tank temperature points in the vertical direction after 3 hours

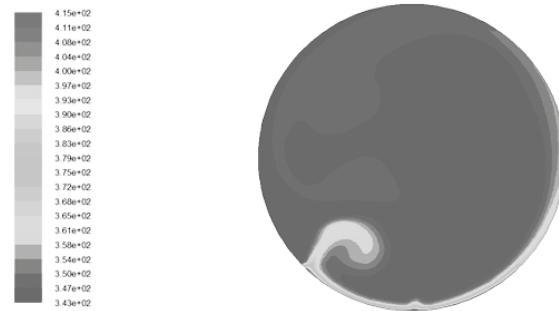


(a)

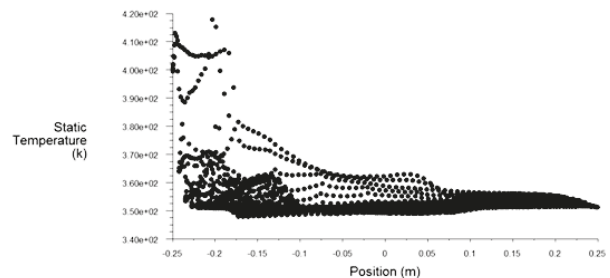


(b)

Fig. 5. (a) Temperature contours inside the tank after 10 minutes (b) Tank temperature plot in the vertical direction after 10 minutes



(a)



(b)

Fig. 7. (a) Temperature contours inside the tank after 6 hours (b) Tank temperature points in the vertical direction after 6 hours

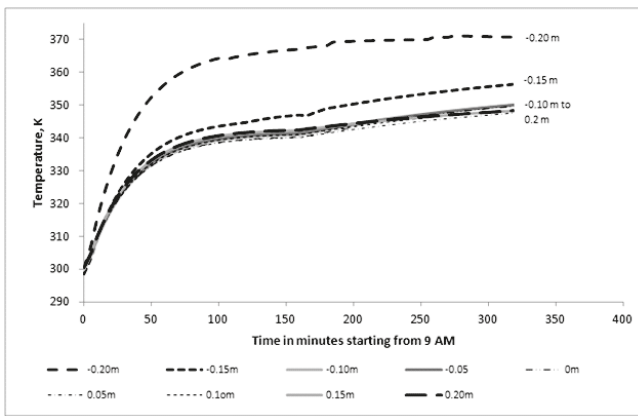


Fig. 8. Temperature profile of the water at different measurement levels at different times starting from 9:00 AM from the experimental data

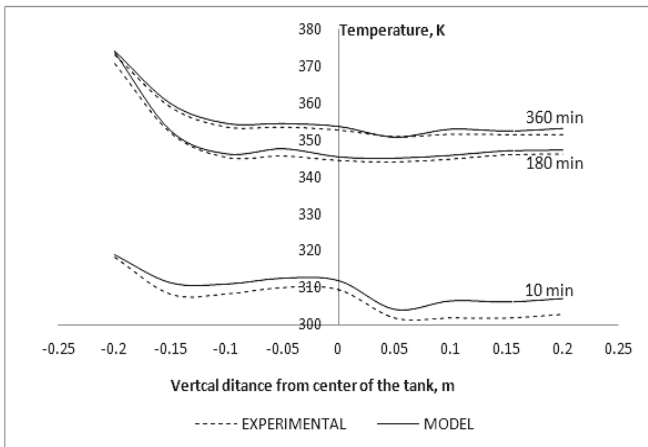


Fig. 9. Comparison of experimental data with results of the model at 9 different levels inside the tank

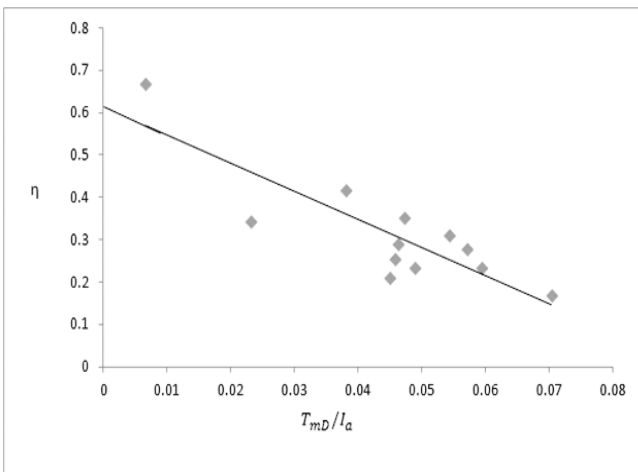


Fig. 10. Mean daily efficiency of the ICS as a function of  $T_{mD} / I_a$

experimental values are in good agreement with the simulation results. Fig.10 gives the mean daily efficiency of the ICS system as a function of  $T_{mD} / I_a$ . Experimental results of 12 different days were used to plot this graph and a linear fit was made with the following equation 8. This equation was used to determine overall the loss coefficient by using the “delta T over I method” as described in Sukatme, 2002. An overall heat loss coefficient of 9.93 W.K-1 was obtained from this method.

It can be seen that the maximum value of efficiency is 0.61. This is comparatively lesser than that reported by Tripanagnostopoulos and Co-Authors (2004) who experimented on ICS systems with the tank enclosed inside the glass covering with involutes shaped and compound parabolic reflectors and obtained the maximum efficiency of 0.71 and 0.67 respectively. The heat loss coefficient during the night was calculated from equation 7 as 20.31 W.K<sup>-1</sup>.

**Conclusion**

An integrated solar collector storage system was tested for its performance and the results were compared with that of the simulation model. The results were found to be in good agreement. The reflectors were located independently as against the conventional method of integrating the reflecting surfaces within the collection system. Comparison of the efficiency with that of conventional integrated collector storage systems showed that this type of arrangement had a very small effect on the thermal efficiency of the system. The maximum average tank temperature obtained was about 350 K. The loss coefficient during the solar absorption period and storage period was higher than conventional systems. However, the low cost of manufacture and installation of this type of system makes it a viable option especially in the low income countries.

**Acknowledgement**

The author acknowledges the support received from the Research Center, College of Engineering, King Saud University, Riyadh, Kingdom of Saudi Arabia, in completing this research work.

**References**

Al-Sanea SA, Zedan MF, Al-Ajlan SA (2004), Adjustment factors for the ASHRAE clear-sky model based on solar-radiation measurements in Riyadh. Applied Energy, 79: 215–237 DOI:10.1016/j.apenergy.2003.11.00.

- David A. Bainbridge (1981), The Integral Passive Solar Water Heater Book, [www.builditsolar.com](http://www.builditsolar.com), 1981 <http://www.builditsolar.com/Projects/WaterHeating/ISPWH/ispwh.htm>.
- Eve Commerford, Patrick L. Gurian and Jin Wen (2008), Design of a Site-Built Integrated Collector Storage Solar Water Heater Under Uncertainty. The Open Renewable Energy Journal, **1**: 17-25 <http://www.benthamscience.com/open/torej/articles/V001/17TOREJ.pdf>.
- Helal, O., Chaouachi, B., Gabsi, S. and Bouden, C. (2010), Energetic Performances Study of an Integrated Collector Storage Solar Water Heater. American J. of Engineering and Applied Sciences, **3**: 152-158 DOI:10.3844/ajeassp.2010.152.158.
- Hamdi Kessentini, Bouden and Chiheb (2013), Numerical and experimental study of an integrated solar collector with CPC reflectors. Renewable Energy, **57**: 577-586. DOI: 10.1016/j.renene.2013.02.015. ISSN: 0960-1481.
- Monia Chaabane, Hatem Mhiri and Philippe Bournot (2011), Numerical Study of an Integrated Collector Storage Solar Water Heater. Journal of Materials Science and Engineering, **B1**: 689-695. DOI: 10.1007/s00231-012-1065-z.
- Rakesh Kumar and Marc. A. Rosen (2010), Thermal performance of integrated collector storage solar water heater with corrugated absorber surface. Applied Thermal Engineering, **30**: 1764 -1768. [http://www.sid.ir/en/VEWSSID/J\\_pdf/1025120110401.pdf](http://www.sid.ir/en/VEWSSID/J_pdf/1025120110401.pdf).
- Smyth, M., Eames, P.C., Norton, B. (2006), Integrated collector storage solar water heaters. Renewable and Sustainable Energy Reviews, **10**: 503-538. DOI:10.1016/j.rser.2004.11.001.
- Souliotis, M., Smyth, M., Tripanagnostopoulos, Y., Zacharopoulos, A., Ramirez, M. and Yianoulis, P. (2011), Heat retaining integrated collector storage solar water heater with asymmetric CPC reflector, **85**: 2474-2487. DOI:10.1016/j.solener.2011.07.005.
- Sridhar, A. and Reddy, K.S. (2007), Transient analysis of modified cuboid solar integrated-collector-storage system. Applied Thermal Engineering, **27**: 330-346 <http://www.sciencedirect.com/science/article/pii/S135943110600278X>.
- Sukatme, S.P. (2002), Solar energy Principles of Thermal Collection and storage, Tata McGraw-Hill Publishing, New Delhi. ISBN (**13**): 978-0-07-026064-1.
- Tripanagnostopoulos, Y. and Souliotis, M. (2004), ICS solar systems with horizontal (E-W) and vertical (N-S) cylindrical water storage tank. Renewable Energy, **29**: 3-96 <http://www.sciencedirect.com/science/article/pii/S0960148105002545>.

*Received: 27 November 2013; Revised: 18 March 2014;  
Accepted: 3 June 2014.*